ASPECTS REGARDING THE QUALITY OF SURFACES OBTAINED BY USING THE SELECTIVE LASER SINTERING TECHNOLOGY

Veronica DESPA [1], Gheorghe I. GHEORGHE [2], Liliana-Laura BĂDIȚĂ [2]

[1] Valahia University of Targoviste,

[2] National Institute of Research and Development for Mechatronics and Measurement Technique, Bucharest

Email: dumiver@yahoo.com

Abstract: *Selective Laser Sintering (SLS) is a rapid prototyping technology useful to provide pieces, assemblies and subassemblies with any geometric complexity, unachievable by other processing methods. The present paper intends to present some aspects regarding the quality of surfaces obtained by this technology. Using methods and techniques of investigation focused on analysis by atomic force microscopy (AFM), the study of two pieces structure made by SLS was realized. These tests have allowed obtaining some qualitative data on porosity as well as some microstructural information of the analyzed areas.*

Keywords: *Selective laser sintering, Atomic force microscopy, Topographic parameters.*

1. INTRODUCTION

Selective Laser Sintering (SLS) is a modern technological process for the manufacture of parts with complex geometry, process mostly used for rapid prototyping and instrumentation.

Technological processes of rapid prototyping by SLS are based on designing and intelligent manufacturing experience gained on stereo-lithography (STL) equipment, but also on the expanding of technological researches on some other special materials groups with mechanical properties closer to the needs of functional assemblies of materials from materials industry or micro-machines constructions (ceramics, ferrous and non-ferrous).

SLS is a family of technological methods that can build a solid body of various types of materials (plastic, metal, ceramic) through solidification of powder material after the successive exposure of powders layers to laser beam of a variety variable powers [1].

Based on the physical properties of used powders, immediately after cessation of laser beam, local solidification takes place almost instantaneously, getting a compact strap, made by directions of molecular chains, surrounded by a volume of powders unexposed to the laser beams.

Thus, we can get pieces, assemblies and subassemblies with any geometric complexity, unachievable by other processing methods. This intelligent technology is used to manufacture designs and prototypes for biomedical implantable products, functional prototypes for automotive and aerospace industry, high quality molds as well as design and static and dynamic testing possibilities of other mechanical pieces for industry.

The technological process is fully automated, it does not require surveillance and the electronic control is achieved by intelligent high-tech equipment. The main advantages are based on the fact that in this advanced technology, tools or specific tools parts are not necessary; metallic pieces are created directly in a single step; the operation is simple;

The complex geometries such as free forms, deep grooves and conformable cooling channels can be produced without an additional effort; un-sintered powder can be reused, providing minimal waste.

A number of different materials are available for use, offering a wide range of industrial applications.

It is about fine powder alloys (e.g. EOS Cobalt-Chrome MP1 - Co, Cr, Mo, Si, Mn, Fe, Ni) which shows excellent mechanical properties (strength, hardness), corrosion resistance and temperature resistance. These alloys are commonly used in biomedical applications, and also for high-temperature engineering applications such as in aero engines. This material is also ideal for many part-building applications such as metallic functional prototypes, individualised products or spares. Pieces made of EOS CobaltChrome MP1 can be proccessed, spark-eroded, welded, polished, and coated if required.

Other available materials are, for example, stainless steel MS1, PH1, Ti64, TiCP [2].

2. EXPERIMENTS

Surfaces of two pieces obtained by SLS were analyzed, the first of which is unprocessed (raw), while the second piece was subsequently polished.

2.1. Used equipment

The metallic parts whose surfaces will be analyzed were realized with EOSINT M270/ PSW3.4 Rapid Prototyping machine at the INCDMTM Institute, Bucharest (fig.1.a) a powerful system used for metals direct laser sintering [2-5]. The process consisted of a single phase, which, realized in this machine, has led to obtain finished pieces by melting the fine metallic powder with a laser beam (fig.1.b). This process is based on three-dimensional CAD data obtained in an earlier design stage.

In order to completely characterize the surfaces of the metallic structures made by SLS method, atomic force microscopy (AFM) was used. Thus, it was used an NTEGRA Probe Nano-Laboratory AFM type, from NT-MDT Moscow, Russia, located in the MEMS & NEMS Laboratory of INCDMTM Bucharest (fig. 2).

a.

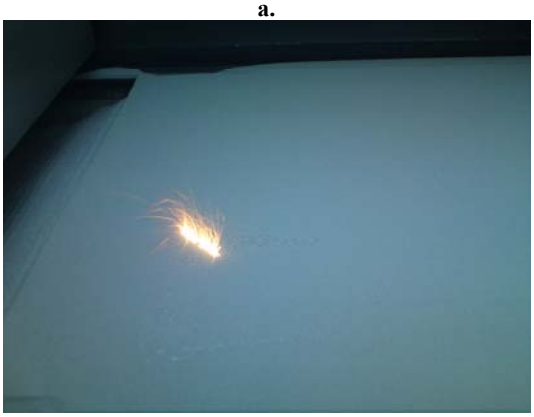

b.

Fig.1. RP machine by SLS EOSINT M270 – INCDMTM Bucharest

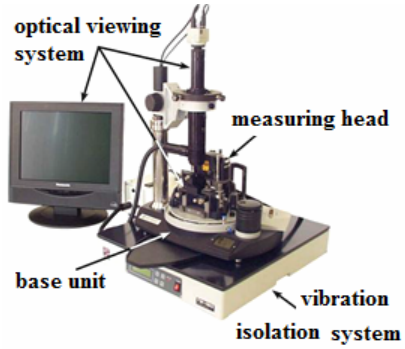

Fig.2. Atomic Force Microscope - NTEGRA Probe NanoLaboratory NT – MDT

The main technical characteristics of this atomic force microscope are:

- Maximum scanning area on X, Y: 50 × 50 µm
- Maximum scanning area on the Z axis: 12 µm
- Plane aberration: max. 2 nm over a horizontal interval of 50 µm, without software corrections
- AFM head with a super-luminescent diode (835 nm)
- Zoom: 780× (for a 19 inch monitor)
- Optical resolution: 1 µm
- High precision digital zoom CCD camera
- Resolution 1032 × 778 pixels
- Frame speed: 20Hz
- Controller processor speed: > 500 MHz

Working principle of AFM is based on the measurement of the interaction force between a tip and the sample's surface using a special measuring probe. The force applied on the tip by the surface leads to the cantilever bending [6-8]. Measuring the deflection of the cantilever, it is possible to assess the interaction force peak - surface.

2.2. Used methods

AFM investigation procedure consisted in identifying and photographing some damaged areas on the arms surface (including base and peak) and the faces of experimentally researched pieces, where were selected areas of 50 x 50 µm.

For each area, analysis of surface topography was performed and topographic parameters were determined using NOVA SPM Software – microscope software [9].

The topographic parameters determined from the AFM study (average roughness S_a, maximum height h_{max}, surface skewness S_{sk}, coefficient of kurtosis S_{ka}) provides information relating to the pieces surfaces.

Surface skewness S_{sk} assesses the asymmetry degree of a distribution and characterizes, together with coefficient of kurtosis S_{ka}, the shape of distribution. Surface skewness S_{sk} is negative or positive, as the survey distribution is asymmetrical to the left or, respectively, right. A symmetrical distribution, such as normal distribution, has zero asymmetry.

Coefficient of kurtosis S_{ka} is part of indices for assessing the form of a distribution. A high coefficient of kurtosis indicates a distribution with large "tails", while a small coefficient of kurtosis shows a distribution in which are present fewer categories far by the mean. If a distribution is close to the normal distribution, Coefficient of kurtosis is around 3. In the case of this analysis, for each scanned area, the average profile in x and y direction was calculated.

3. RESULTS

3.1. Analysis of the laser sintered piece and unprocessed

On the basis of the surfaces identified by the AFM CCD camera were selected few areas of some damaged areas of the arm 1 (including base and peak) of unprocessed piece, presented in Fig. 3.

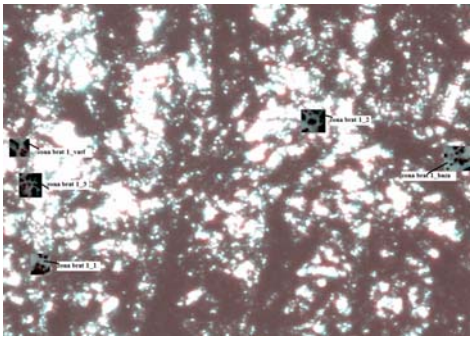

Fig.3.a. Image of some damaged areas

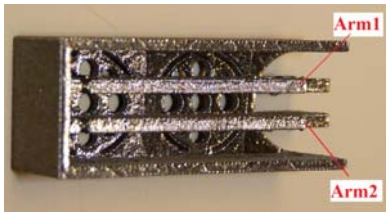

Fig.3.b. Image of the unprocessed piece surfaces

In these areas the AFM topographic analysis was done at the nanometric level. Fig. 4 shows an example from the AFM analysis results for different areas on the surface of the arm no. 1 of unprocessed piece.

Arm 1 (unprocessed piece).
Topographic parameters experimentally determined

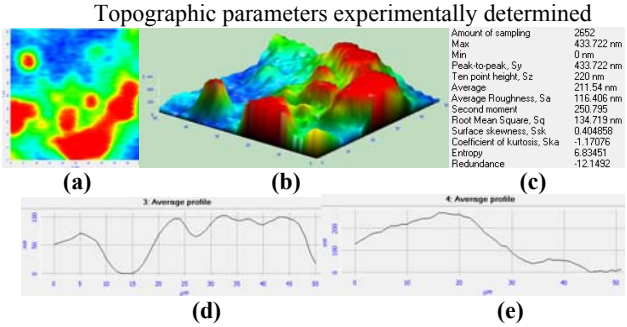

Fig.4. AFM analysis of the area 1 surface of the first arm of the unprocessed piece: (a) scanned 2D surface, (b) scanned surface converted into a 3D, (c) topographic parameters, (d) average profile in the x direction, (e) average profile in the y direction.

It is similar preceded, analysing using AFM, the surfaces from the base, respectively, the peak of the first arm of the unprocessed piece.

Summarizing the results of experimental researches made in laboratory, in Table 1 values of the main topographic parameters experimentally determined and their average value calculated for the first arm of the unprocessed piece are presented.

Table 1. Values of the main topographic parameters experimentally determined and their average value calculated for the first arm of the unprocessed piece.

No. (experiment arm 1)	R_a (nm)	h_{max} (nm)	S_{sk}	S_{ka}
Arm 1_1	116.406	433.722	0.404	-1.170
Arm 1_2	123.496	429.084	-0.169	-1.423
Arm 1_3	134.672	463.874	-0.180	-1.393
Arm 1_base	116.356	536.736	0.925	-0.194
Arm 1_peak	120.709	414.435	-0.729	-0.979
Average value calculated	**122.327**	**455.570**	**0.0502**	**-1.031**

Similarly to the first arm analysis, were identified areas where some domains of some damaged areas of arm 2 were selected (including the base and tip) on the unprocessed piece. Synthesis of the laboratory experimental research is presented in Table 2, which shows the values of the main topographic parameters experimentally determined and their average value calculated for the arm 2 of the unprocessed piece.

Table 2. Values of the main topographic parameters experimentally determined and their average value calculated for the second arm of the unprocessed piece.

No. (experiment arm 2)	R_a (nm)	h_{max} (nm)	S_{sk}	S_{ka}
Arm 2_1	143.679	537.789	0.391	-1.111
Arm 2_2	122.635	448.829	0.240	-1.405
Arm 2_3	91.304	579.477	1.355	1.714
Arm 2_base	141.014	507.576	0.465	-1.205
Arm 2_peak	124.334	474.342	0.225	-1.376
Average value calculated	**124.593**	**509.602**	**0.535**	**-0.676**

3.2. Analysis of the laser sintered piece and processed (polished)

Based on the areas identified by the AFM CCD camera several parts of damaged areas from arm 1 of the processed piece were selected, shown in Fig. 5. In these areas topographic AFM analysis was realized at nanometric level.

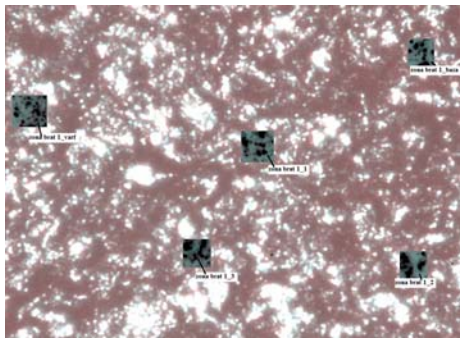

Fig.5.a. Images of some damaged areas

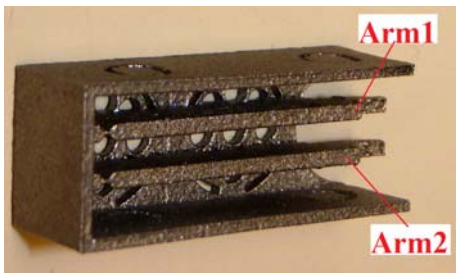

Fig.5b. Images of the processed piece surfaces

Figure 6 shows an example of AFM analysis results for the surface of arm 1 of the processed (polished) piece.

As in the case of unprocessed piece, using AFM, surfaces of some areas from the arm 1 of the processed piece were analyzed. Following the experimental researches, values of the main topographic parameters experimentally determined and their average value calculated for the first arm of the processed piece are synthesized (Table 3).

Arm 1 (processed piece).
Topographic parameters experimentally determined

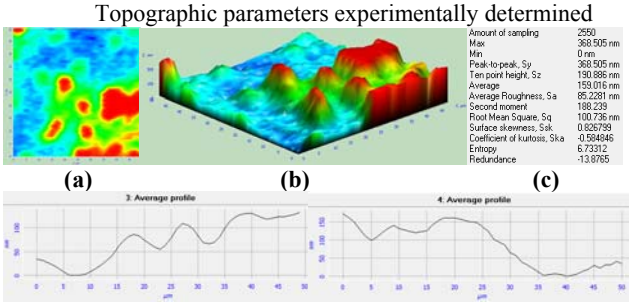

Fig.6. AFM analysis of the area 1 surface of the first arm of the processed piece: (a) the scanned 2D surface, (b) scanned surface converted into a 3D, (c) determined topographic parameters, (d) the average profile in the x direction, (e) the average profile in the y direction.

Table 3. Values of the main topographic parameters experimentally determined and their average value calculated for the first arm of the processed piece.

No. (experiment arm 1)	R_a (nm)	h_{max} (nm)	S_{sk}	S_{ka}
Arm 1_1	85.228	368.505	0.826	-0.584
Arm 1_2	64.144	378.057	2.044	3.376
Arm 1_3	95.468	369.497	0.705	-0.836
Arm 1_base	78.594	340.337	0.935	-0.323
Arm 1_peak	88.076	374.594	0.313	-1.166
Average value calculated	**82.302**	**366.198**	**0.964**	**0.0934**

Similarly to the first arm analysis, were identified areas where some domains of some damaged areas of arm 2 were selected on the processed piece.

Synthesizing the laboratory experimental research Table 4 shows the values of the main topographic parameters experimentally determined and their average value calculated for the arm 2 of the processed piece (polished).

Table 4. Values of the main topographic parameters experimentally determined and their average value calculated for the second arm of the processed piece.

No. (experiment arm 2)	R_a (nm)	h_{max} (nm)	S_{sk}	S_{ka}
Arm 2_1	89.438	354.208	0.557	-0.944
Arm 2_2	112.357	383.914	0.364	-1.393
Arm 2_3	92.339	375.143	0.260	-1.075
Arm 2_base	122.413	359.686	-0.022	-1.713
Arm 2_peak	52.862	398.932	1.312	1.666
Average value calculated	**93.881**	**374.376**	**0.494**	**-0.6918**

The images obtained by AFM scanning show various irregularities that can be seen as more or less pronounced, and also particles torn from the surface or scratches. There are, however, uniform areas and areas with almost no defects. Table 5 presents the average values of the main topographic parameters experimentally determined corresponding to the surfaces of the two analysed parts: the raw part, and the processed one.

Table 5. Average values of the main topographic parameters for the surfaces of the two pieces

	Unprocessed piece				Polished piece			
	R_a (nm)	h_{max} (nm)	S_{sk}	S_{ka}	R_a (nm)	h_{max} (nm)	S_{sk}	S_{ka}
Arm 1	122.327	455.570	0.050	-1.031	82.302	366.198	0.964	0.093
Arm 2	124.593	509.602	0.535	-0.676	93.881	374.376	0.494	-0.691
Face 1	122.433	572.381	0.444	-0.628	77.985	342.565	0.626	-0.568
Face 2	116.768	463.306	0.495	-0.707	67.96	324.684	0.9	0.476
Face 3	122.045	559.850	0.534	-0.374	80.243	333.165	0.445	-0.834

4. CONCLUSIONS

Thus, the experimental study conducted by investigations carried out through atomic force microscopy - AFM - on samples of two pieces of the same material (CoCrMo alloy), but having different roughness (one piece is raw, while the second was grinded), there was a significant variation in the two types of surface roughness. The main conclusions arising from this research work are:

- Grinding the surfaces of the pieces is shown primarily by the fact that the average value h_{max} decreases from 500 nm to 350 nm mean value (as a result of the removal of material from the surface through the laser sintering process).
- R_a decreases also along with the processing from average values of 120 nm to average values of 80 nm, while the surface becomes smoother, less rough.
- S_{sk} has positive averages, which indicates an asymmetric pool distribution to the right. Considering that these values are less than zero, but less than 1, these distributions pools could be regarded as very close to symmetry.
- S_{sa} has a sall value in both cases, indicating that fewer groups are present far from average. Excess has negative values for all surfaces characterized, indicating a platicurtic distribution (and this means that the curve is flat).
- The roughness is smaller; the surface is smoother, more suitable for further micro-mecatronics micro-manipulation applications.

- Taking into account the issues raised, in order to obtain a better piece topographically through laser sintering technology, it is useful to perform an operation processing to improve surface quality: sanding, dry and wet abrasive blasting, spherical hardening shot blasting (shot peening), electro-chemical polishing, manual polishing and so on. Therefore, the research work has demonstrated that the experimental polishing is a suitable process for this purpose.
- These results obtained in this study show the possibility to eliminate the disadvantage of the surface non-uniformity of piece obtained by this technology.

REFERENCES

[1]. Gh. Gheorghe, D. Ciobota, I. Drstvensek, The new generation of rapid prototyping technology in selective laser sintering for metal powders, The Romanian Review Precision Mechanics, Optics & Mechatronics, Nr.35/2009, ISBN:1584 -5982.

[2]. Gh. Gheorghe s.a., Advanced Microtechnologies by the rapid prototyping with selective laser sintering, Ed. CEFIN, Bucharest, 2010.

[3]. Gh. Gheorghe, L. Bădiță, V. Despa, D. Ciobotă, Micro-nanometrologically and topographic characterization of metallic pieces surfaces obtained by laser sintering, Digest Journal of Nanomaterials and Biostructures, Vol.8, No.3, July-September 2013, p.1037-1041;

[4]. A. Voicu, Gh. I. Gheorghe, L. Bădiță, A. Cirstoiu, 3D Measuring of Complex Automotive Parts by Multiple Laser Scanning, Applied Mechanics and Materials Vol. 371 (2013) pp. 519-523.

[5]. V. Despa, A. Catangiu, D.N. Ungureanu, I.A. Ivan, Surface structure of CoCrMo and Ti6Al4V parts obtained by selective laser sintering, Journal of Optoelectronics and Advanced Materials (JOAM)/ISSN 1454-4164, Vol.15. ISS.7-8/2013, pp. 858-862.

[6]. *http://en.wikipedia.org/wiki/Atomic_force_microscopy*

[7]. D.L. Bourell et al., Selective Laser Sintering of Metals, Proceedings of ASME, New York: American Society of Mechanical Engineers, 1994, pp. 519–528.

[8]. H.J. Butt, B. Cappella, M. Kappl., Force measurements with the atomic force microscope: Technique, interpretationand applications, Surface science reports, Vol. 59, Issues 1–6, October 2005, pp. 1–152.

[9]. F. L. Leite, L. H. Mattoso, O. N. Oliveira, S. P. Herrmann, The Atomic Force Spectroscopy as a Tool to Investigate Surface Forces: Basic Principles and Applications, Formatex 2007, pp. 747 -757.